

# Using the CW-Complex to Represent the Topological Structure of Implicit Surfaces and Solids.

John C. Hart  
School of EECS  
Washington State University  
Pullman WA 99164-2752  
(509) 335-2343  
hart@eecs.wsu.edu

## Abstract

We investigate the CW-complex as a data structure for visualizing and controlling the topology of implicit surfaces. Previous methods for controlling the blending of implicit surfaces redefined the contribution of a metaball or unioned blended components. Morse theory provides new insight into the topology of the surface a function implicitly defines by studying the critical points of the function. These critical points are organized by a separatrix structure into a CW-complex. This CW-complex forms a topological skeleton of the object, indicating connectedness and the possibility of connectedness at various locations in the surface model. Definitions, algorithms and applications for the CW-complex of an implicit surface and the solid it bounds are given as a preliminary step toward direct control of the topology of an implicit surface.

## 1 Introduction

The holy grail of implicit surface modeling research is the control of blending. Most implicit surface primitives blend based on nothing more than proximity, often blending in undesirable locations. Current solutions have created new implicit primitives that do not blend, or use blending graphics that can create unsightly creasing.

Blending usually changes the topology of the surface, so we turn to tools from topology to analyze the unwanted blending problem. Morse theory shows how the topology of a surface implicitly defined by a function can be discerned by the arrangement of function's critical points. A theorem from Morse theory describes a structure that represents the topology of the surface called the CW-complex. We therefore propose using the CW-complex as a data structure for representing the topological structure of implicit surfaces. We present algorithms for computing the embedding of the CW-complex on an implicit surface and within an implicit solid.

## 2 The Unwanted Blending Problem

The implicit surfaces most in need of attention to topology is the metaball or blobby model. This model consists of spheres blended by adding quasi-Gaussian three-dimensional bump functions centered at key points in space. As the blending

of these metaballs depends primarily on proximity, unwanted blending often occurs. For example, a hand can be constructed from metaballs by blending fingers with a palm. However, if the tips of any two fingers get too close to each other, then they too will blend together.

Gascuel [1993] showed how to simulate *precise contact* between implicit surfaces. (The following summary is a gross simplification, and, for example, omits all details of physical modeling and propagation regions.) If the implicit surface of  $f_i$  comes into contact with the surface of  $f_j$ , then the resulting deformation on  $f_i$  is given by

$$g_i(\mathbf{x}) = f_i(\mathbf{x}) - f_j(\mathbf{x}). \quad (1)$$

The metaball of  $f_j$  has been replaced with a negative metaball of  $-f_j$  to determine the effect on metaball of  $f_i$ . A similar range deformation occurs on metaball  $j$ . The resulting implicit surfaces of  $g_i$  and  $g_j$  may touch but can not interpenetrate, for if any point  $\mathbf{x}$  we have  $g_i(\mathbf{x}) > 0$  then  $f_i(\mathbf{x}) > f_j(\mathbf{x})$  and therefore  $g_j < 0$ . Precise contact modeling provides a method for preventing blending and even interpenetration between two proximate metaballs, but can deforms the metaballs even if they do not intersect.

Guy & Wyvill [1996] proposed a blending graph to control the blending of metaballs. (The following summary focuses only on controlling the blending, and omits the precise contact component.) The blending graph  $G$  is a graph that contains a vertex for every metaball, and an edge  $(i, j)$  denoting that metaballs  $i$  and  $j$  should blend together. Hence for each metaball function  $f_i$ , a new function is defined as

$$g_i(\mathbf{x}) = f_i(\mathbf{x}) + \sum_{(i,j) \in G} f_j(\mathbf{x}). \quad (2)$$

The resulting implicit surface is then the union (CSG, not blended) of the implicit surfaces of the  $g_i$

$$G(\mathbf{x}) = \max_i g_i(\mathbf{x}). \quad (3)$$

This union operation results in creases in the implicit surfaces due to the  $C^1$  discontinuities introduced by the *max* operation. These discontinuities could be removed by replace the maximum with an *R-function* representation [Pasko *et al.*, 1995] but this could reintroduce unwanted blending.

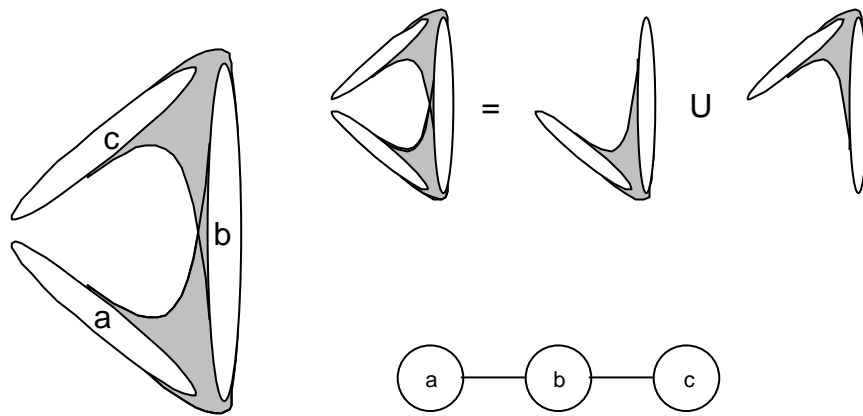


Figure 1: The blend graph controlling the blending of three meta-ellipses.

### 3 Morse Theory

The blending of metaballs, intentional or not, is a change in the topological type of the shape. Hence we use techniques from topology to analyze the problem of unwanted blending. We base our analysis on Morse theory, which describes the topology of surfaces by the configuration of critical points, and use a data structure from algebraic topology called the CW-complex to represent the relationship of critical points and the topological structure of the surface.

We assume surfaces are defined in *general position*, such that form of the surface remains unchanged after a perturbation of the surface's parameters. The assumption of general form means that there may be special cases in which this paper's claims do not hold and its algorithms malfunction, but such cases are isolated in the parameter space of the surface and may be removed by perturbing these parameters.

Let  $f$  be a smooth real function on a smooth manifold  $M^1$ . The *critical points* of  $f$  are the points  $p \in M$  where its gradient  $\nabla f(p)$  vanishes. The *critical value* is the value of  $f$  at a given critical point.

The Hessian  $V(p)$  of  $f$  at  $p \in M$  yields a square symmetric matrix of second derivatives of  $f$ . Let  $\lambda_i$  denote the  $i$ th eigenvalue, in order of non-decreasing value, and let  $\mathbf{v}_i$  denote its corresponding eigenvector. Critical points are classified by the number of negative eigenvalues of this matrix. The function  $f$  is called a *Morse function* if the Hessian is nonsingular for every  $p \in M$ . If any of these eigenvalues are zero, then the critical point is *degenerate*. We assume the surface model is sufficiently parameterized such that these degeneracies are special cases and can be removed via perturbation.

Morse theory provides a connection between the arrangement of these critical points and the topology of  $M$  [Milnor, 1963]. For example, let  $0$  be a regular value of  $g : \mathbb{R}^3 \rightarrow \mathbb{R}$ . Then by the implicit function theorem, its inverse image  $g^{-1}(0)$  is a manifold and is called the implicit surface of  $g$ .

<sup>1</sup>Note that with special care, Morse theory can be applied to manifolds of continuity as low as  $C^0$  [Goresky & MacPherson, 1988] and for functions of continuity as low as  $C^1$  [Hart *et al.*, 1998].

Let  $f$  be a *height function* on  $g^{-1}(0)$  such that  $f(x, y, z) = y$ . Then  $f$  is a Morse function. Using a classic example of Bott, let  $g^{-1}(0)$  be a torus encircling the  $z$ -axis. Then there exist four critical points such that

$$\nabla f = (0, 1, 0) \cdot \nabla g = \partial g / \partial y \quad (4)$$

vanishes: one minimum at the bottom of the torus, one maximum at the top of the torus, and two saddle points on the top and bottom of the hole. If we were to construct the torus from the bottom up, we see that a component of the surface was created at the minima, opposing sections of the surface joined at the saddles, and the surface closed at the top.

If the manifold is  $\mathbb{R}^3$ , then Morse theory can be used to define the topology of the implicit solid of  $f$  [Hart, 1998; Fomenko & Kunii, 1997]. Critical points are classified in four categories: maxima (3-saddles), 2-saddles, 1-saddles and minima (0-saddles)<sup>2</sup>. For implicit surfaces constructed with metaballs, the critical points occur at key locations defining the topology of the surface. A maxima occurs near the center of a metaball component<sup>3</sup>. A component is created if this critical value is positive, and is destroyed if it is negative. A 2-saddle occurs between pairs of metaballs. These metaballs are connected if this critical value is positive, and are disconnected if it is negative. A 1-saddle occurs in the middle of a ring of three or more metaballs. This ring is filled if this critical value is positive, and is pierced if it is negative. A minimum occurs inside a non-planar collection of four or more metaballs. The collection solid if this critical value is positive, but contains an air bubble if the critical value is negative.

### 4 The CW-Complex

In algebraic topology, specifically homotopy theory, shapes are often constructed out of cells of different dimension. An

<sup>2</sup>Johnson *et al.* [1999] called the critical points of real functions on  $\mathbb{R}^3$  *peaks, passes, pales and pits*.

<sup>3</sup>Stander & Hart [1997] provides an example where ellipsoidal metaballs can blend to yield an additional disjoint "phantom" component.

$n$ -cell is denoted  $e^n$  and represents a building block of dimension  $n$ . For example, a 0-cell is a point, a 1-cell is a space curve segment, a 2-cell is a surface patch and a 3-cell is a solid. The  $n$ -cells are closed such that the space curve segment includes its endpoints, the patch includes its boundary curve and the solid includes its boundary surface.

Each  $n$ -cell is homeomorphic to the  $n$ -ball

$$B^n = \{\mathbf{x} \in \mathbb{R}^n : \|\mathbf{x}\| \leq 1\}. \quad (5)$$

This homeomorphism also maps the *boundary of a  $n$ -cell* to the  $(n - 1)$ -sphere defined

$$S^n = \{\mathbf{x} \in \mathbb{R}^n : \|\mathbf{x}\| = 1\}. \quad (6)$$

It is helpful to note that  $S^{-1} = \emptyset$  and this boundary (from algebraic topology) is not the same as the boundary from point-set topology (closure minus interior).

We can now construct a *CW-complex* out of  $n$ -cells of increasing dimensions. An  $n$ -cell is attached to a CW-complex by *identifying* the boundary of the cell with the union of some collection of  $(n-1)$ -cells in the complex.

Hence, we can construct a 3-dimensional CW-complex. We begin with the empty set. We then attach 0-cells by unioning disjoint points into the set. We attach 1-cells by unioning space curve segments whose endpoints lie on these points. We attach 2-cells by unioning surface patches whose boundaries lie on the space curve segments. We attach 3-cells by filling in closed regions bounded by space curves.

Note that the CW-complex generalizes the notion of a graph by adding cells of dimension greater than 1. Also note that a CW-complex generalizes the notion of a simplicial complex in that triangles become "polygons" and tetrahedra become "polyhedra." Note also that the cells need not be straight, such that a "polygon" may contain as few as a single edge connecting a single vertex to itself, and a "polyhedron" may contain as few as a single face, a single vertex and no "edges."

A theorem [Milnor, 1963] from classical Morse theory states that a compact manifold has the homotopy type of a CW-complex consisting of a  $\lambda$ -cell for each critical point of type  $\lambda$  for a given Morse function. The proof of this theorem is based on the analogous operations of attaching a handle to a manifold and attaching a  $\lambda$ -cell to a CW-complex. The remainder of this paper describes how this CW-complex may be instead constructed from the separatrix structure connecting the critical points to each other.

## 5 The CW-Complex of an Implicit Surface

As before let  $g$  implicitly define the surface  $g^{-1}(0)$  and let  $f$  be a Morse function on the surface. Let  $\mathbf{x}_i$  be the critical points of  $f$  on  $g^{-1}(0)$ , and let  $c_i = f(\mathbf{x}_i)$  be the corresponding critical values.

The 0-cells of the CW-complex exist at the minima of the surface. The 1-cells are separatrix curves constructed by integrating the ordinary differential equation

$$\dot{\mathbf{x}} = \pm \mathbf{v}_0(\mathbf{x}) \quad (7)$$

with the initial values set to the saddle points, and termination values set to the minima. Situations where this curve leads

from a saddle to another saddle are unstable and removed via perturbation.

The 2-cells are the remaining components of the implicit surface, and can be interrogated using, for example, surface particles [Witkin & Heckbert, 1994]. Each of these remaining components will contain a single maximum which can be used as the seed point for the birth of a surface particle population. These surface particles can be further constrained to never cross a separatrix curve.

Figure 2 demonstrates the procedure on a torus. Note that if the surface contains a single minimum, the resulting CW-complex is a "bouquet" and is easily "unfolded" into its fundamental polygon [Fomenko & Kunii, 1997]. This form of the CW-complex provides a representation of the topology of the surface embedded on the surface itself.

## 6 The CW-Complex of an Implicit Solid

Likewise, one may compute the CW-complex of an implicit solid.

0-cells of the CW-complex are placed on the maxima. Separatrix curves are traced through each 2-saddle by integrating the ordinary differential equation

$$\dot{\mathbf{x}} = \pm \mathbf{v}_2(\mathbf{x}) \quad (8)$$

until they reach the maxima. Note that these separatrix curves can not stably reach any critical point other than a maxima.

We again use surface particles to interrogate the 2-cells of the CW-complex. The surface particles are spawned from the 1-saddles, and remain on the separatrix surface by the constraint

$$\dot{\mathbf{x}} \cdot \mathbf{v}_0(\mathbf{x}) = 0. \quad (9)$$

The surface particles are further constrained to not cross the boundaries of the separatrix curves defined earlier.

The 3-cells are now well defined as the compact spatial regions bounded by the separatrix surfaces, and each 3-cell will contain a single minima critical point. These regions could be interrogated by any volumetric region growing method.

Note that we have reversed the dimension of the cells with respect to the index of the critical points (e.g. a 0-cell corresponds to an index 3 critical point — a maximum). This is an artifact of the sign convention of metaballs disagreeing with the sign convention of Morse theory. Note that the cell dimension would agree with the critical point index for the function  $-f$  which has an identical implicit surface, and also the same solid if the interior is defined for negative values instead of positive values.

Figure 3 demonstrates the CW-complex of a cuboid constructed from 8 metaballs, along with several implicit surfaces of the function for different isovalues. The critical structure includes 8 maxima at the vertices of the cube, 12 2-saddles centered along the edges of the cube, 6 1-saddles centered on the faces of the cube and a single minima at the centroid of the cube. The CW-complex thus contains 8 0-cells connected by 12 1-cells filled by 6 2-cells surrounding a single 3-cell.

The data structure described by this paper was also devised and used to represent crystal atomic structures [Johnson *et al.*, 1999; Johnson, 1999]. In fact, the Gaussian electron density

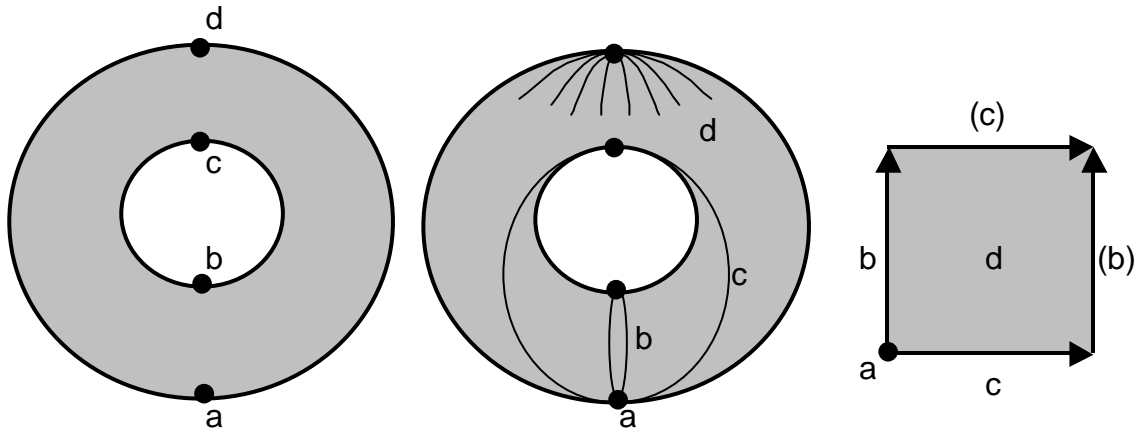


Figure 2: The CW-complex of a torus.

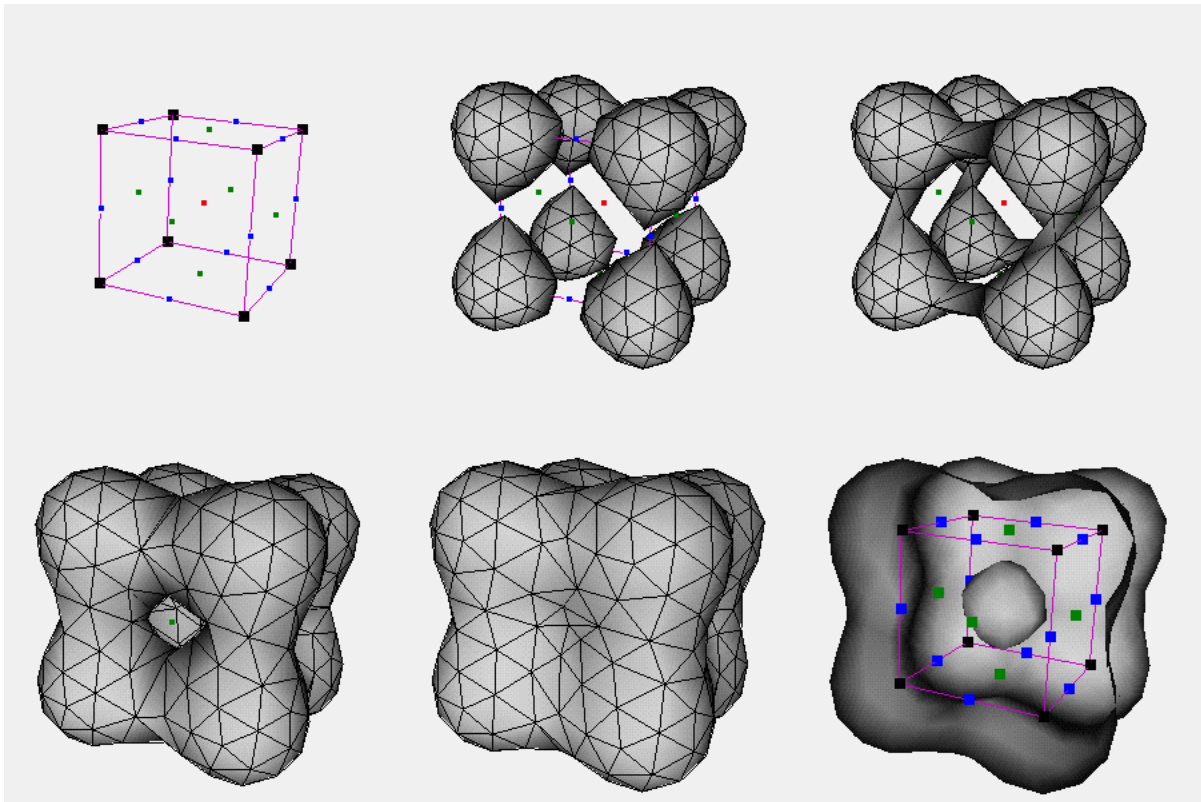


Figure 3: The CW-complex of a cuboid implicit solid.

maps used in crystallography are precisely the blobby objects we use in implicit surface modeling [Blinn, 1982]. The structure appearing in Figure 3 is the very same one [Johnson *et al.*, 1999] used to represent the topology of the crystalline structure of salt.

For implicit surfaces, the CW-complex corresponding to the defining function forms a skeletal structure. Whereas the medial-axis skeleton represents the geometry of the shape, the CW-complex skeletonizes the topology of the shape. Depending on the sign of the critical values, the components of the CW-complex can be drawn to better indicate their effect on the topology of the implicit surface. A 0-cell indicates a connected component surrounding a maxima, and can be represented by a small circle that is filled if the maxima's value is positive, or unfilled if it is negative. A 1-cell indicates a possible connection between components, and can be represented by a solid curve segment if the value of the corresponding 2-saddle is positive, or by a dashed segment if it is negative. A 2-cell indicates a region surrounded by a ring of metaballs, and can be represented by a hashing of solid lines if the value of the 1-saddle it contains is positive, or by a dotted surface if it is negative. A 3-cell indicates a region surrounded by a shell of metaballs, and can be represented by the patches on its boundary. These patches are brightly shaded if the value of the minima it surrounds is positive, or dimly shaded if it is negative.

We can replace the metaball kernel sum function  $f$  with a distance function

$$h(\mathbf{x}) = \text{sgn}(f(\mathbf{x})) \min\{\|\mathbf{x} - \mathbf{y}\| \mid \mathbf{y} \in f^{-1}(0)\} \quad (10)$$

which shares the same sign and implicit surface as  $f$ . Then we hypothesize that the CW-complex constructed from the separatrix structure of this new function  $h$  is the medial-axis skeleton of the implicit surface. Note that this implies that the CW-complex of  $h$  never contains a minima, for it would then contain a 3-cell which would have been further "eroded" by the medial axis transform.

An alternative to the CW-complex for representing the critical structure is the *critical net* [Johnson *et al.*, 1999; Johnson, 1999]. The critical net is a simple graph representation of the separatrix structure of the critical points. This graph consists of a vertex for each critical point of any type. These vertices are connected by edges that indicate a separatrix connection between the critical points. A simple straight edge connects the separatrices between 2-saddles and maxima points. A separatrix curve can be extended from a 1-saddle to a 2-saddle by integrating

$$\dot{\mathbf{x}} = \pm \mathbf{v}_1(\mathbf{x}). \quad (11)$$

An edge replaces this curve connecting the vertices representing the 1-saddle and the 2-saddle. Similarly, a separatrix curve can be extended from the 1-saddle to the minimum by integrating

$$\dot{\mathbf{x}} = \pm \mathbf{v}_0(\mathbf{x}) \quad (12)$$

and replacing the separatrix curve by a straight edge between the vertices corresponding to the 1-saddle and the minimum.

## 7 Conclusion

The CW-complex of an implicit surface replaces the smooth surface with a quasi-polygonal version that can provide a sim-

pler representation of otherwise complex surfaces. In some cases, the CW-complex can be embedded in the plane providing further insight into the connectedness of the surface.

The CW-complex of an implicit solid displays the topology of the implicit surface to the user. Current controls would only allow the user to adjust the position, orientation or scale of metaballs. We envision a system that allows the user to directly control the topology of the implicit surface by application of range deformations that only change the sign of a specified critical point, but do not change the locations or number of the critical points.

The algorithms described focused on 2-manifold surfaces and 3-manifold solids. The techniques might also be helpful to understand the topology of higher dimensional manifolds. For example, in computer graphics, the bidirectional reflectance distribution function (BRDF) used for modeling local illumination is the 4-manifold defined as the explicit surface (graph) of the function  $\rho(\theta_i, \phi_i, \theta_r, \phi_r)$  with the identification  $\rho(\theta_i, \phi_i, \theta_r, \phi_r) = \rho(\theta_r, \phi_r, \theta_i, \phi_i)$ . A better understanding of the topology of this 4-manifold might lead to more efficient representations of it. Similarly, the plenoptic function used in image-based modeling and rendering also describes a 4-manifold whose topological understanding could lead to more efficient implementation.

This research was funded by a grant by the National Science Foundation. The author is grateful to fellow faculty members Ulrike Axen for discussions on the CW-complex and locating otherwise obscure references, and Bob Lewis for discussions on applications of computational topology to modeling illumination.

## References

- [Blinn, 1982] Blinn, J. F. A generalization of algebraic surface drawing. *ACM Transactions on Graphics* 1(3), July 1982, pp. 235–256.
- [Fomenko & Kunii, 1997] Fomenko, A. T. and Kunii, T. L. *Topological Modeling for Visualization*. Springer, 1997.
- [Gascuel, 1993] Gascuel, M.-P. An implicit formulation for precise contact modeling between flexible solids. In *Computer Graphics (Annual Conference Series.)*, Aug. 1993, pp. 313–320. Proc. SIGGRAPH 93.
- [Goresky & MacPherson, 1988] Goresky, M. and MacPherson, R. *Stratified Morse Theory*. Springer, April 1988.
- [Guy & Wyvill, 1996] Guy, A. and Wyvill, B. Controlled blending for implicit surfaces using a graph. In Proc. *Implicit Surfaces '95*. Eurographics, 1996, pp. 107–112.
- [Hart *et al.*, 1998] Hart, J., Durr, A., and Harsch, D. Critical points of polynomial metaballs. In *Proc. Workshop on Implicit Surfaces*. Eurographics/SIGGRAPH, June 1998, pp. 69–76.
- [Hart, 1998] Hart, J. C. Morse theory for implicit surface modeling. In Hege, H.-C. and Polthier, K., eds., *Mathematical Visualization*, pp. 257–268. Springer-Verlag, Heidelberg, 1998.

- [Johnson *et al.*, 1999] Johnson, C., Burnett, M., and Dunbar, W. Crystallographic topology and its applications. In Bourne, P. and Watenpaugh, K., eds., *Crystallographics Computing 7: Proceedings from the Macromolecular Crystallography Computing School*. University Press, 1999.
- [Johnson, 1999] Johnson, C. K. Crystallographic topology 2: Overview and work in progress. In Alexiades, V. and Siopis, G., eds., *Trends in Mathematical Physics*, pp. 275–306. AMS/International Press, 1999.
- [Milnor, 1963] Milnor, J. *Morse Theory*, vol. 51 of *Annals of Mathematics Studies*. Princeton University Press, Princeton, NJ, 1963.
- [Pasko *et al.*, 1995] Pasko, A., Adzhiev, V., Sourin, A., and Savchenko, V. Function representation in geometric modeling: concepts, implementation and applications. *The Visual Computer* 11(8), 1995, pp. 429–446.
- [Stander & Hart, 1997] Stander, B. T. and Hart, J. C. Guaranteeing the topology of an implicit surface polygonization for interactive modeling. In *Computer Graphics (Annual Conference Series)*, Aug. 1997, pp. 279–286.
- [Witkin & Heckbert, 1994] Witkin, A. P. and Heckbert, P. S. Using particles to sample and control implicit surfaces. In *Computer Graphics (Annual Conference Series)*, July 1994, pp. 269–277.